

## RESEARCH ARTICLE

# Lipocalin 2 binds to membrane phosphatidylethanolamine to induce lipid raft movement in a PKA-dependent manner and modulates sperm maturation

Hitomi Watanabe<sup>1,\*</sup>, Toru Takeo<sup>2,\*</sup>, Hiromasa Tojo<sup>3,\*</sup>, Kazuhito Sakoh<sup>2</sup>, Thorsten Berger<sup>4</sup>, Naomi Nakagata<sup>2</sup>, Tak W. Mak<sup>4</sup> and Gen Kondoh<sup>1,‡</sup>

## ABSTRACT

Mammalian sperm undergo multiple maturation steps after leaving the testis in order to become competent for fertilization, but the molecular mechanisms underlying this process remain unclear. In terms of identifying factors crucial for these processes *in vivo*, we found that lipocalin 2 (*Lcn2*), which is known as an innate immune factor inhibiting bacterial and malarial growth, can modulate sperm maturation. Most sperm that migrated to the oviduct of wild-type females underwent lipid raft reorganization and glycosylphosphatidylinositol-anchored protein shedding, which are signatures of sperm maturation, but few did so in *Lcn2* null mice. Furthermore, we found that LCN2 binds to membrane phosphatidylethanolamine to reinforce lipid raft reorganization via a PKA-dependent mechanism and promotes sperm to acquire fertility by facilitating cholesterol efflux. These observations imply that mammals possess a mode for sperm maturation in addition to the albumin-mediated pathway.

**KEY WORDS:** LCN2, Sperm, Lipid raft, Phosphatidylethanolamine, PKA, Oviduct, Mouse

## INTRODUCTION

After leaving the testis, mammalian sperm acquire various modifications in the male and female reproductive tracts in order to complete fertilization competency. Capacitation is one of the most important steps in the sperm maturation process, which occurs in the female reproductive tract and is possibly affected by humoral factors and/or the interaction between the sperm and the oviductal epithelium (Yanagimachi, 2009; Ikawa et al., 2010; Smith and Yanagimachi, 1990). During capacitation, the sperm outer membrane undergoes cholesterol depletion, which is associated with signaling processes such as protein kinase A (PKA) activation toward protein tyrosine phosphorylation (Visconti et al., 1995; Travis and Kopf, 2002; Visconti, 2009; Bailey, 2010; Signorelli et al., 2012). Another important step is the acrosome reaction (AR) (Wassarman and Litscher, 2001, 2008). The acrosome is a Golgi-derived organelle that overlies the sperm nucleus in the apical region of the sperm head. During the AR, the outer acrosomal membrane

and the plasma membrane of sperm fuse, followed by exposure of the inner acrosomal membrane and the release of acrosomal components. Zona pellucida (ZP) binding of the sperm is a trigger of the AR *in vivo* and this process can be experimentally mimicked by treating sperm with calcium ionophore to facilitate Ca<sup>2+</sup> influx (Costello et al., 2009). Only sperm that have completed the AR can exclusively penetrate the ZP and fuse with the egg plasma membrane.

In a previous study, we discovered the linkage between ganglioside GM1 relocation and glycosylphosphatidylinositol-anchored protein (GPI-AP) release (Watanabe and Kondoh, 2011). GM1 is a characteristic component and reliable biomarker of the lipid raft. However, bovine serum albumin (BSA), which is widely used for inducing sperm capacitation, alone could not induce GM1 relocation nor GPI-AP release, but could following calcium ionophore A23187 treatment, implying that these molecular movements are completed when the AR occurs (Watanabe and Kondoh, 2011).

In terms of identifying female factors that induce such molecular movements *in vivo*, we find that lipocalin 2 (LCN2) can promote sperm capacitation. LCN2 is a small extracellular protein that belongs to the lipocalin family (Flower, 1996; Åkerstrom et al., 2000). It is also well known as an innate immune factor that captures the siderophore, a molecular complex crucial for bacterial iron uptake, and suppresses bacterial growth (Goetz et al., 2002; Flo et al., 2004; Berger et al., 2006). More recently, LCN2 was shown to suppress bloodstream malarial growth by activating both innate and adaptive immune systems via an iron metabolism-reinforcing function (Zhao et al., 2012).

In this study, we found that GM1 relocation/GPI-AP release of the sperm membrane was strongly suppressed in the *Lcn2* knockout female reproductive tract. LCN2 protein could induce GM1 relocation in a PKA-dependent manner and also cholesterol efflux, and was able to facilitate the AR in association with Ca<sup>2+</sup> influx and also the fertility of sperm *in vitro*, which are known parameters for sperm capacitation. Moreover, we discovered that LCN2 directly binds to membrane phosphatidylethanolamine (PE). These *in vivo* and *in vitro* observations indicate that LCN2 modulates fertility acquisition in sperm.

## RESULTS

### Identification of LCN2 in female uterotubular junction

To induce sperm maturation for the acquisition of fertility, BSA or methyl- $\beta$ -cyclodextrin (M- $\beta$ -CD) is commonly used, but these are artificial compounds. We aimed to identify *in vivo* factors that have a similar function to these compounds. For one trial, we compared the gene expression profiles of female uterotubular junction (UTJ) tissues, where sperm maturation is believed to begin, among three

<sup>1</sup>Laboratory of Animal Experiments for Regeneration, Institute for Frontier Medical Sciences, Kyoto University, Kyoto 606-8507, Japan. <sup>2</sup>Division of Reproductive Engineering, Center for Animal Resources and Development, Kumamoto University, Kumamoto 860-0811, Japan. <sup>3</sup>Department of Biochemistry and Molecular Biology, Graduate School of Medicine, Osaka University, Suita, Osaka 565-0871, Japan. <sup>4</sup>The Campbell Family Institute for Breast Cancer Research and the Ontario Cancer Institute, University Health Network, Toronto, Ontario, Canada M5G 2C1.

\*These authors contributed equally to this work

‡Author for correspondence (kondohg@frontier.kyoto-u.ac.jp)

different statuses: status 1, estrous without mating; status 2, estrous mated with vasectomized males; and status 3, estrous mated with normal males. When we compared status 1 with status 2, or status 1 with status 3, elevations of multiple immune reaction genes were observed (data not shown). Then, we set up a comparison between status 2 and status 3. The main difference between them is that status 3 contains sperm or epididymal component stimuli, whereas status 2 does not; thus, we could detect changes of the gene expression profile directed by sperm. We found 210 genes with elevated expression in status 3 (supplementary material Table S1).

Aiming to find UTJ environmental factors, we searched in particular for soluble or membrane-attached proteins. Among these, we first focused on LCN2. Its expression was elevated more than 6-fold by copulation stimuli and ~3-fold by sperm/epididymal component stimuli (supplementary material Table S1). LCN2 protein expression in UTJ was confirmed by immunoblotting and was significantly elevated by these stimuli (supplementary material Fig. S1). Moreover, it is reported that *Lcn2* knockout females show a significant reduction in pregnancy rate (Berger et al., 2006) (supplementary material Fig. S3), which prompted us to examine LCN2 further.

### LCN2 is a sperm maturation factor in the oviduct

First, EGFP (K268Q)-GPI transgenic males, a mouse strain that can be used to monitor GPI-AP release, were mated with *Lcn2* knockout females; then, migrating sperm were collected from oviducts and examined for GM1 and EGFP (K268Q)-GPI statuses. We observed that GM1 relocation (Fig. 1A) or shedding of EGFP (K268Q)-GPI in the sperm head (Fig. 1B) was suppressed in the absence of *Lcn2* (Fig. 1C,D). Considering our previous investigations (Watanabe and Kondoh, 2011), these observations suggested that LCN2 is a candidate sperm maturation factor in the female reproductive tract.

### LCN2 promotes sperm capacitation *in vitro*

To understand the molecular mechanisms underlying LCN2-mediated sperm maturation, we prepared recombinant LCN2 protein (supplementary material Fig. S2) and performed further analyses *in vitro*. In a previous study, it was reported that LCN2 is expressed in the epididymis (Elangovan et al., 2004). Thus, to exclude epididymal LCN2 and examine LCN2 functions quantitatively by adjusting the protein concentration, we used *Lcn2* knockout mouse sperm in the following studies. This mouse shows normal *in vitro* (see Fig. 3) or *in vivo* (supplementary material Fig. S3) fertility. When the epididymal *Lcn2*<sup>-/-</sup> sperm were treated with 40 µg/ml LCN2, which is one-hundredth of the amount of BSA in a standard treatment (4 mg/ml), GM1 relocation was significantly induced (Fig. 2A), an early phase signature of capacitation (Watanabe and Kondoh, 2011). However, neither the AR, as detected by IZUMO1 relocation, nor GPI-AP release (Watanabe and Kondoh, 2011; Satouh et al., 2012) was induced by LCN2 alone (Fig. 2B; supplementary material Fig. S4). BSA is not an inducer of the AR by itself but induces capacitation, which is required to prepare sperm for the AR (Watanabe and Kondoh, 2011). Incubation of sperm with LCN2 can prepare sperm for A23187-induced AR (Fig. 2C,D). These lines of evidence imply that LCN2 is a capacitation-promoting factor.

### GM1 movement by LCN2 depends on a PKA-mediated mechanism, but not PI3K, the Raf-MAP kinase pathway nor protein tyrosine phosphorylation

One of the most rapid intracellular events following the induction of capacitation is the activation of PKA. It occurs within 30 min of induction, followed by other events such as phosphoinositide

3-kinase (PI3K) activation, Raf-MAP kinase signaling pathway activation or protein tyrosine phosphorylation (Visconti, 2009; Signorelli et al., 2012). We first examined the involvement of PKA in GM1 movement. Sperm were incubated in LCN2-containing medium supplemented with the PKA inhibitor KT5720, and stained with AlexaFluor 594-conjugated cholera toxin subunit B (CTB). As shown in Fig. 2E, relocation of GM1 by LCN2 was suppressed upon PKA inhibition. By contrast, the PI3K inhibitor AS605240 had no effect.

Then, the manner of downstream signaling events was examined. After incubating sperm with BSA, protein tyrosine phosphorylation is induced (Bailey, 2010). We examined this after LCN2 treatment,

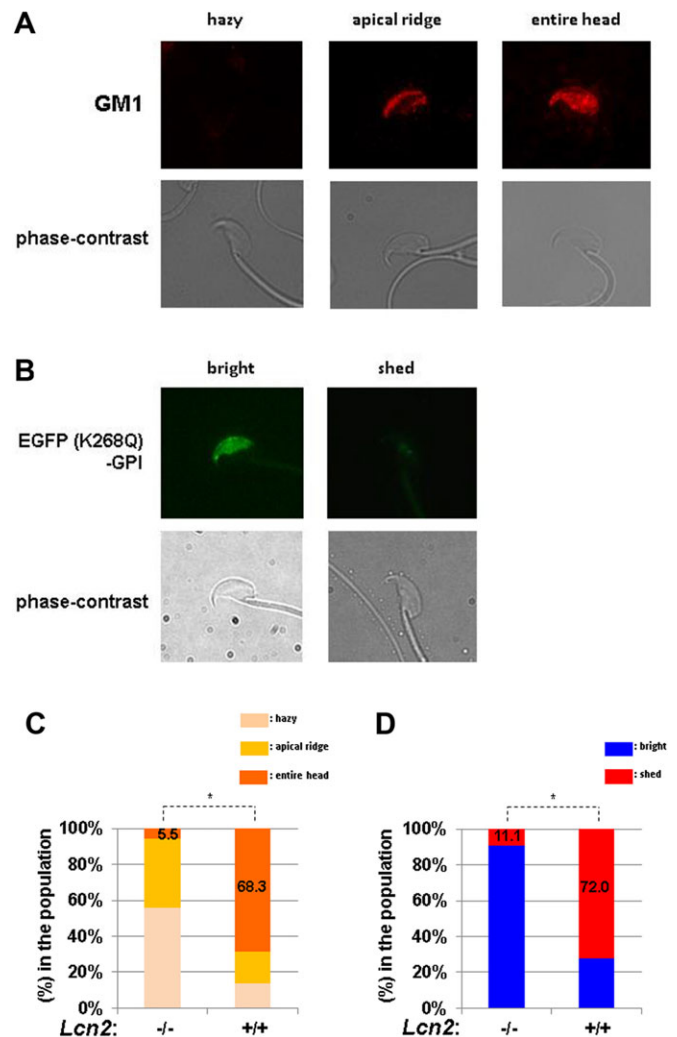


**Fig. 1. LCN2 is a sperm maturation factor in the mouse female reproductive tract.** (A) GM1 staining of migrating EGFP (K268Q)-GPI transgenic sperm collected from oviducts. Sperm classified according to three patterns (hazy, apical ridge, entire head) (Watanabe and Kondoh, 2011) are displayed. (B) EGFP (K268Q)-GPI migrating sperm collected from oviducts. Sperm classified according to two patterns (bright, shed) (Watanabe and Kondoh, 2011) are displayed. (C) GM1 staining patterns among the population of ejaculated EGFP (K268Q)-GPI transgenic sperm collected from oviducts of *Lcn2* knockout mice. Data from wild-type mice (*Lcn2*<sup>+/+</sup>) are also displayed. Number of sperm examined: *Lcn2*<sup>-/-</sup>, *n*=161; *Lcn2*<sup>+/+</sup>, *n*=158. \**P*<0.001, Student's *t*-test. (D) EGFP (K268Q)-GPI staining patterns among the population. Number of sperm examined: *Lcn2*<sup>-/-</sup>, *n*=161; *Lcn2*<sup>+/+</sup>, *n*=154. \**P*<0.005, Student's *t*-test. Values in bars indicate the percentage of sperm showing the entire head pattern (C) or the shed pattern (D). Data were accumulated from five independent experiments.

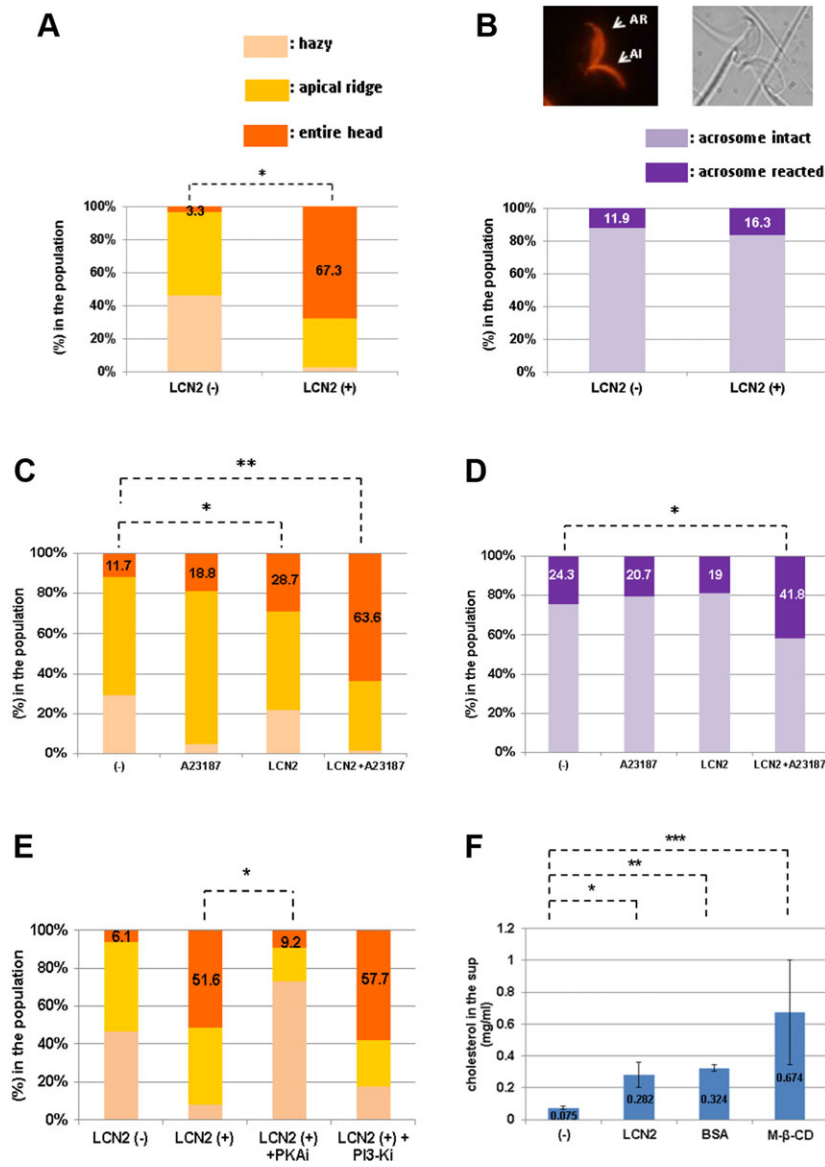


**Fig. 2. LCN2 mode for sperm maturation *in vitro*.** (A) GM1 relocation. Sperm collected from the epididymis of *Lcn2*<sup>-/-</sup> males were incubated in HTF-PVA medium with (+) or without (-) LCN2 for 120 min and stained with AlexaFluor 594-conjugated CTB. Sperm were classified according to the three patterns (Fig. 1A) and their proportion in the population determined. Number of sperm examined: LCN2 (-), *n*=210; LCN2 (+), *n*=215. \**P*<0.0005, Student's *t*-test. (B) IZUMO1 immunostaining for evaluating the acrosome reaction. Acrosome-reacted sperm (AR) showed the entire head staining pattern, whereas acrosome-intact sperm showed an acrosomal cap pattern (AI). Number of sperm examined: LCN2 (-), *n*=218; LCN2 (+), *n*=233. (C) GM1 status after A23187 calcium ionophore treatment to induce AR. Epididymal sperm were preincubated in HTF-PVA or HTF-PVA-LCN2 (40 μg/ml) for 120 min and then further incubated with A23187 for 60 min. Number of sperm examined: HTF-PVA (-), *n*=196; HTF-PVA+A23187 (A23187), *n*=191; HTF-PVA-LCN2 (LCN2), *n*=202; HTF-PVA-LCN2+A23187 (LCN2+A23187), *n*=209. Student's *t*-test: \**P*<0.005, \*\**P*<0.01. ANOVA: *P*<0.05. (D) IZUMO1 status after A23187 calcium ionophore treatment. Number of sperm examined: HTF-PVA (-), *n*=214; HTF-PVA+A23187 (A23187), *n*=203; HTF-PVA-LCN2 (LCN2), *n*=205; HTF-PVA-LCN2+A23187 (LCN2+A23187), *n*=273. Student's *t*-test: \**P*<0.01. ANOVA: *P*<0.003. (E) GM1 relocation was inhibited by PKA inhibitor but not by PI3K inhibitor. *Lcn2*<sup>-/-</sup> sperm were incubated in LCN2-containing medium supplemented with 1.0 μM KT5720 (PKAi), 5.0 μM AS605240 (PI3-Ki) or vehicle only for 120 min and stained with AlexaFluor 594-conjugated CTB. Data from medium lacking LCN2 are also indicated. Sperm classified according to the three patterns are indicated by their proportion in the population examined. Number of sperm examined: LCN2 (-), *n*=229; LCN2 (+), *n*=225; LCN2 (+)+PKAi, *n*=238; LCN2 (+)+PI3-Ki, *n*=239. Student's *t*-test: \**P*<0.01. ANOVA: *P*<0.001. (F) LCN2 facilitates cholesterol efflux from the sperm membrane. Sperm collected from the epididymis were cultured in HTF-PVA (-), HTF-LCN2 (LCN2), HTF-BSA (BSA) or HTF-M-β-CD (M-β-CD) for 120 min. Culture supernatants were collected and the amount of cholesterol was measured. Student's *t*-test: \**P*<0.001, \*\**P*<0.0001, \*\*\**P*<0.05. ANOVA: *P*<0.0001. Values in bars indicate the percentage of sperm showing the entire head pattern (A,C,E), percentage acrosome-reacted sperm (B,D), or mg/ml cholesterol (F). Data were accumulated from four (A-C,E) or three (D,F) independent experiments.

but found no induction, even with an excess amount, in contrast to BSA or M-β-CD (supplementary material Figs S5 and S6). Moreover, we found that Raf kinase inhibitor protein (RKIP) was downregulated in BSA-treated or M-β-CD-treated sperm, suggesting activation of the Raf-MAP kinase signaling pathway (Minden et al., 1994), but this did not occur in LCN2-treated sperm (supplementary material Fig. S5). These observations suggest that

LCN2-mediated lipid raft movement is mediated by PKA action, but, unlike BSA or M-β-CD, does not depend on downstream signaling events.

### LCN2 can induce cholesterol efflux

Next, we examined whether LCN2 can facilitate cholesterol efflux, a well-known phenomenon in sperm capacitation. As shown in

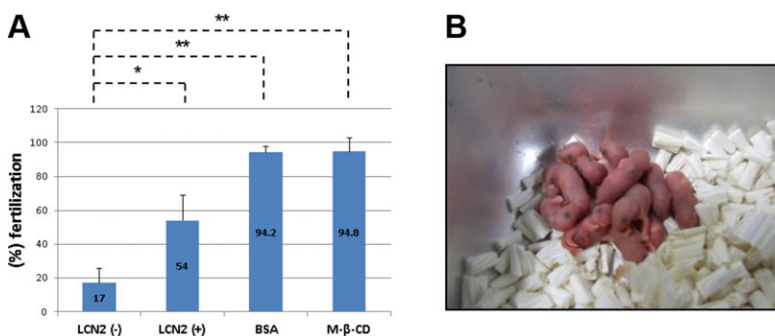


**Fig. 3. *In vitro* fertility of LCN2-treated sperm.** (A) Epididymal sperm were preincubated in HTF-PVA or HTF-PVA-LCN2, HTF-BSA or HTF-PVA-M-β-CD for 120 min and then inseminated with cumulus-positive oocytes in HTF-PVA. Efficiency of IVF is indicated as percentage fertilization (see Materials and Methods). Five (HTF-PVA, HTF-PVA-LCN2) or four (HTF-BSA, HTF-PVA-M-β-CD) independent experiments were performed. Number of eggs examined: LCN2 (-), *n*=160; LCN2 (+), *n*=171; BSA, *n*=131; M-β-CD, *n*=128. Student's *t*-test: \**P*<0.005, \*\**P*<0.0001. ANOVA: *P*<0.0001. (B) Newborn pups obtained from embryos fertilized in the presence of LCN2 appear normal.



Fig. 2F, marked cholesterol efflux was observed, confirming that LCN2 induces capacitation. Notably, LCN2 could again remove cholesterol at a similar efficiency to the 100-fold greater amount of BSA present in a standard treatment.

### LCN2 promotes *in vitro* fertilization

We then examined the effect of LCN2 on *in vitro* fertilization (IVF). As shown in Fig. 3A, LCN2 possesses the ability to increase IVF efficiency. Moreover, when embryos obtained from LCN2-mediated IVF were transferred to pseudo-pregnant females, normal pups (Fig. 3B) were obtained in reasonable numbers (129 newborns after 299 embryos transferred).

### LCN2 binding to sperm membrane induces lipid raft movement

To clarify the biological significance of LCN2 binding to the sperm membrane, we treated epididymal sperm with biotinylated LCN2 and monitored for LCN2 binding and lipid raft movement over the same timecourse. LCN2 binding was first detectable after 30 min of incubation (Fig. 4A,C). More than 80% of LCN2-bound sperm showed GM1 staining throughout the sperm head. By contrast, almost all LCN2-deficient sperm showed a hazy pattern (Fig. 4B). When sperm were incubated for up to 120 min, the number of LCN2-bound sperm increased in a time-dependent manner (Fig. 4C). In the same timecourse, GM1 staining throughout the entire head sperm increased (Fig. 4D), implying that LCN2 induces GM1 movement as soon as it binds to the sperm surface.

### LCN2 binds to membrane PE

To clarify the exact LCN2 capacitation process, we searched for hydrophobic molecules captured by LCN2. LCN2 was first contacted with a membrane spotted with multiple plasma membrane lipids, and its specific binding to PE was detected (Fig. 5A). Notably, LCN2 did not bind to cholesterol, suggesting that it cannot capture cholesterol, in contrast to BSA. In this assay, the blot of PE was rather heterogeneous. To investigate whether this might have been caused by the presence of multiple PE species in the spot, we used synthetic mono-PE molecules in the following studies. First, we undertook examinations with representative membrane PE, dipalmitoyl PE (PPPE) or palmito-oleyl PE (POPE). When we spotted PEs at a series of concentrations and contacted them with LCN2, we found that LCN2 bound to PPPE, but not to POPE, in a dose-dependent manner (Fig. 5B; supplementary material Fig. S7). Again, LCN2 did not bind to cholesterol, even at high concentration. Then, we compared multiple PE species, including PPPE, POPE, distearoyl PE (SSPE) and lyso PE (LPE), and found that LCN2 specifically bound to PE in which both acyl chains are saturated, such as PPPE and SSPE, suggesting the requirement for a saturated acyl chain in the *sn*-2 position of PE for binding (Fig. 5C).

Next, we examined whether LCN2 binds to sperm membrane via PE. Recombinant LCN2 was conjugated with biotin, contacted to the sperm and detected with fluorescently labeled streptavidin. LCN2 bound to the sperm membrane (Fig. 5D, middle), which was consistent with a previous report (Elangovan et al., 2004). This binding of LCN2 was suppressed by cinnamycin, a peptide toxin

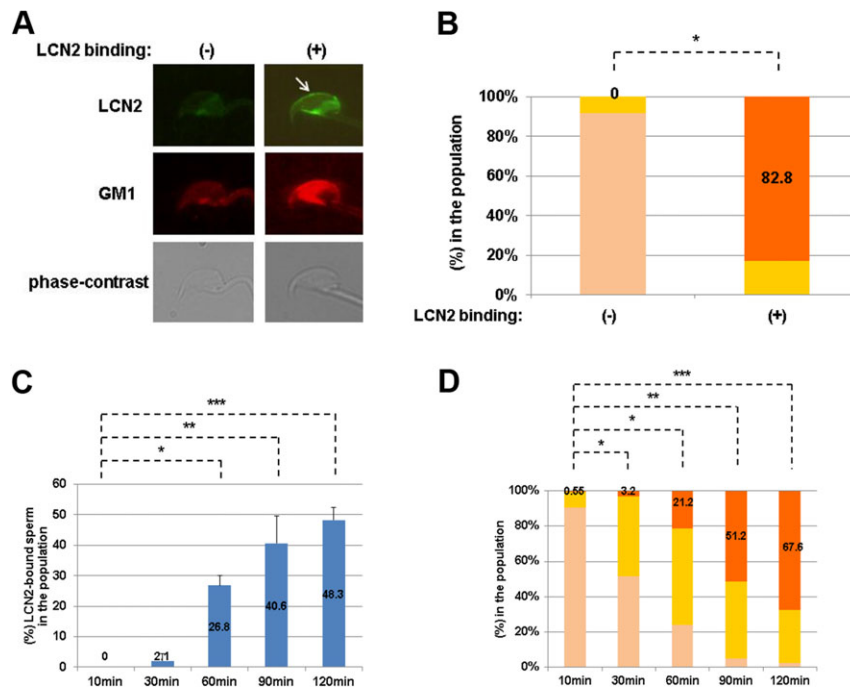


**Fig. 4. Binding of LCN2 to the sperm surface.** (A) (Top) Representative LCN2 binding patterns. Arrow indicates LCN2 binding on sperm membrane. (Middle) GM1 was localized by staining with AlexaFluor 594-conjugated CTB. (Bottom) Phase-contrast views. (B) GM1 staining patterns combined with LCN2 binding to the sperm surface. Sperm were classified with regard to the three patterns and are indicated by their proportion among the population examined. Number of sperm examined: LCN2 binding (-),  $n=166$ ; LCN2 binding (+),  $n=157$ .  $*P<0.0001$ , Student's *t*-test. (C) Timecourse study of LCN2 binding to the sperm surface. *Lcn2*<sup>-/-</sup> sperm were incubated with 40  $\mu\text{g/ml}$  biotinylated recombinant LCN2 for the indicated time and LCN2 binding was detected with AlexaFluor 488-conjugated streptavidin. LCN2-bound sperm are indicated by their proportion in the population examined. Number of sperm examined: 10 min,  $n=210$ ; 30 min,  $n=223$ ; 60 min,  $n=234$ ; 90 min,  $n=287$ ; 120 min,  $n=271$ .  $*P<0.0005$ ,  $**P<0.005$ ,  $***P<0.0001$ , Student's *t*-test. (D) Timecourse study of GM1 staining patterns. Sperm in C were stained with AlexaFluor 594-conjugated CTB at the same time. Sperm classified according to the three patterns are indicated by their proportion among the population examined. Number of sperm examined: 10 min,  $n=181$ ; 30 min,  $n=190$ ; 60 min,  $n=203$ ; 90 min,  $n=221$ ; 120 min,  $n=238$ .  $*P<0.05$ ,  $**P<0.005$ ,  $***P<0.0001$ , Student's *t*-test. Values in bars indicate the percentage of sperm showing the entire head pattern (B,D) or percentage LCN2-bound sperm (C). Data were accumulated from three independent experiments (B-D).

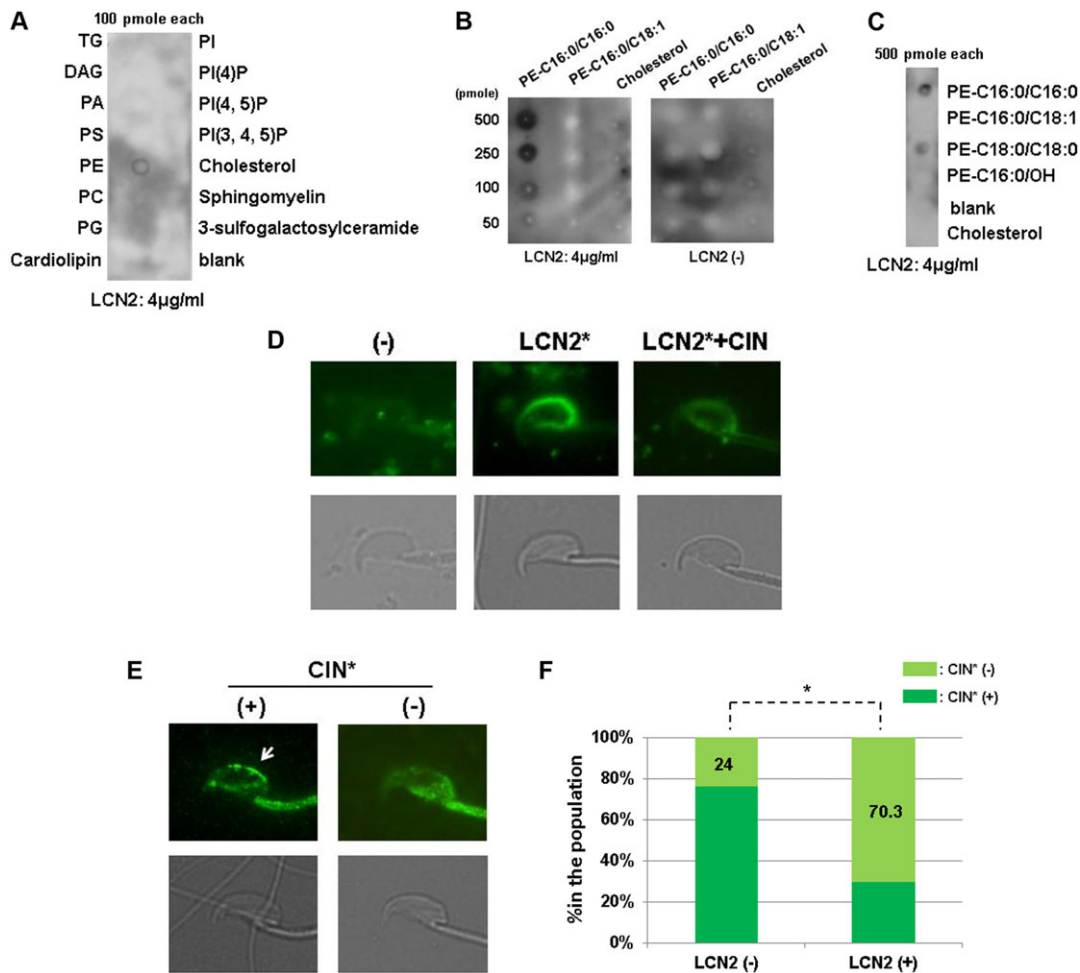


**Fig. 5. LCN2 binds to membrane PE.** (A) First screening for LCN2 binding to plasma membrane lipids. Multiple membrane lipids were spotted on the membrane and contacted with LCN2. TG, triglycerol; DAG, diacylglycerol; PA, phosphatidic acid; PS, phosphatidylserine; PE, phosphatidylethanolamine; PC, phosphatidylcholine; PG, phosphatidylglycerol; PI, phosphatidylinositol. (B) Dose-dependent manner of PPPE (PE-C16:0/C16:0) binding to LCN2. Each lipid was spotted on the membrane at the indicated dose. LCN2 did not bind to POPE (PE-C16:0/C18:1) or cholesterol, even at a high dose. (C) PE species-specific binding of LCN2. LCN2 preferentially binds to PE carrying a saturated acyl chain in the *sn*-2 position, such as PPPE (PE-C16:0/C16:0) or SSPE (PE-C18:0/C18:0). (D) LCN2 binding to sperm is mediated by PE. Biotin-conjugated LCN2 (LCN2\*) was applied to sperm samples and detected with fluorescently labeled streptavidin. In the presence of excess cold cinnamycin (CIN), LCN2\* binding was suppressed. (-), Control staining without LCN2. Lower panels are phase-contrast views. (E) Binding of cinnamycin on the sperm surface. Biotin-conjugated cinnamycin was applied to sperm samples and detected with AlexaFluor 488-conjugated streptavidin. Both cinnamycin binding-positive (+) and cinnamycin binding-negative (-) sperm exist in the population. Arrow indicates cinnamycin binding on the sperm surface. (F) Binding of cinnamycin was competed by LCN2 on the sperm surface. *Lcn2*<sup>-/-</sup> sperm were incubated with or without LCN2 for 120 min, fixed with methanol, stained with biotinylated cinnamycin and detected with AlexaFluor 488-conjugated streptavidin. Sperm classified with regard to the two patterns in E are indicated by their proportion among the population examined. Number of sperm examined: LCN2 (-),  $n=179$ ; LCN2 (+),  $n=185$ . Data from three independent experiments were accumulated. Values in bars indicate percentage cinnamycin (-) sperm. \* $P<0.01$ , Student's *t*-test.

derived from *Streptomyces* that specifically binds to PE (Zhao, 2011; Makino et al., 2003), indicating that LCN2 binds to sperm membrane via PE, and possibly PPPE or SSPE (Fig. 5C).

Furthermore, we examined whether LCN2 binding to PE competes with cinnamycin. After incubating sperm in HTF-PVA or HTF-PVA-LCN2 followed by fixing with methanol, biotin-conjugated cinnamycin was applied and detected with fluorescently labeled streptavidin. The majority of sperm without LCN2 treatment showed cinnamycin binding, whereas sperm treated with LCN2 were abrogated for this binding (Fig. 5E,F), confirming that LCN2 binds directly to PE.

## DISCUSSION

It was reported that sperm that undergo AR prior to ZP binding are more likely to fertilize successfully (Jin et al., 2011). Thus, acrosome-reacted sperm in the oviduct might be favorable for fertilization

*in vivo*. The number of such sperm is diminished in *Lcn2* knockout oviduct, indicating that LCN2 could lead the majority of migrating sperm to complete the maturation process prior to ZP binding. Previously, it was demonstrated that LCN2 suppresses the AR and IVF induced by BSA (Lee et al., 2005). According to this observation, LCN2 might also suppress the albumin-mediated capacitation pathway *in vivo*. As shown in Fig. 1, sperm that migrated to the oviduct lacking LCN2 exhibited neither GM1 relocation nor GPI-AP release (see *Lcn2*<sup>-/-</sup> columns), which are signatures of BSA-mediated capacitation; although the pregnancy rate of these females was lower than in the wild type, a comparable number of pups could be obtained (Berger et al., 2006) (supplementary material Fig. S3). This might be explained by a compensation mechanism mediated by albumin. When LCN2 is absent, the albumin-mediated capacitation pathway might become active, followed by the ZP-induced AR (supplementary material Fig. S8).

Moreover, GPI-AP shedding was observed *in vivo* but not *in vitro* (compare Fig. 1D and supplementary material Fig. S4). However, both GM1 and IZUMO1 relocations were reinforced by A23187 treatment (Fig. 2C,D), suggesting that other *in vivo* factors might cooperate with LCN2 to facilitate sperm maturation. To test one possibility, we treated sperm with LCN2 in the presence of progesterone (Coy et al., 2012), an AR-inducing factor, but found no cooperative effects (data not shown). Therefore, *in vivo* factors that facilitate LCN2-mediated sperm maturation remain to be identified in future studies.

Here, we also discovered that LCN2 directly binds to PE, particularly highly hydrophobic species. A previous report described that LCN2 binds to the sperm surface, and is then internalized and distributed throughout the cytosol (Elangovan et al., 2004). It is well known that PE is a major phospholipid of the inner leaflet of the plasma membrane, but is present in low quantities in the outer leaflet, leading to the asymmetric localization of phospholipid. Previously, it was reported that a capacitating agent, bicarbonate, causes collapse of this asymmetric localization via a PKA-dependent mechanism and some PE remains in the outer leaflet (Gadella and Harrison, 2000). Thus, it is possible that capacitation induced by bicarbonate exposes PE to the sperm surface and leads to LCN2 binding. A rapid intracellular event after the induction of capacitation is the activation of PKA, which occurs within 30 min of induction. Since lipid raft movement induced by LCN2 is also PKA dependent and starts soon after LCN2 binding to the sperm surface, bicarbonate and LCN2 might cooperatively facilitate the early phase of capacitation.

However, LCN2 action is not PI3K dependent and cannot induce protein tyrosine phosphorylation nor activate the Raf-MAP kinase pathway, which are late events (~120 min) after PKA activation. These reactions are linked to hyperactivation of sperm motility (Visconti, 2009; Signorelli et al., 2012). Therefore, LCN2 is only required for lipid raft movement in the sperm head, but is not necessary to induce late events in the sperm flagellum. Since LCN2 induces cholesterol efflux and AR with calcium ionophore, it can prepare the sperm head membrane for ZP binding or egg fusion to complete fertilization (Fig. 3A).

Although the machinery for the AR is conserved from primitive animals to mammals, capacitation is specific to animals in which fertilization occurs in the female reproductive tract (Yanagimachi, 1988). Sperm and components of semen are foreign agents for females. Indeed, we observed the host defense machinery of the female reproductive tract dealing with them in the same way as with microbes (supplementary material Table S1). However, mammalian sperm seem to have adapted to this environment and utilize *in situ* factors to achieve full fertilization ability. Our findings might provide the first evidence of cross-talk between the innate immune and reproductive systems.

## MATERIALS AND METHODS

### Microarray analysis

Total RNA samples were prepared from UTJ tissues of ten CD-1 females with three different statuses: (1) estrous without mating; (2) estrous mated with vasectomized males; (3) estrous mated with normal males. Gene expression profiles were compared between statuses 1 and 2, 1 and 3, or 2 and 3 using a microarray system (Agilent Technologies). Data are deposited in Gene Expression Omnibus (GEO) under accession number GSE56620. A total of 210 genes exhibiting more than double expression in status 3 compared with status 2 were identified.

### Preparation of recombinant LCN2 protein

*Lcn2* cDNA was obtained by reverse transcription (RT)-PCR using mouse uterus cDNA as a template and the following primer pair: 5'-TGAATTCACCATGGCCCTGAGTGTGTCATGTGCTGG-3' and 5'-GTGGAATTCATCACTTATCATCATCATCTTATAATCGTTGTCATGTCATTTGGTCG-3'.

This encodes a C-terminal FLAG-tagged version of LCN2 protein (LCN2-FLAG). The CAAG vector, which was cleaved with *EcoRI* followed by blunt-ending, was ligated with the PCR product. Transfected CHO cells were cultured with CD OptiCHO protein-free chemically defined medium (Life Technologies) and the culture supernatant collected. Recombinant LCN2 protein was captured using an anti-FLAG M2-agarose affinity column (Sigma) and eluted from the column using 0.1 mg/ml FLAG peptide (Sigma). The peak fraction of recombinant protein was collected and excess FLAG peptide removed using a Microcon Ultracel YM-10 centrifugal filter device (Millipore). Purity of the protein was examined by SDS-PAGE followed by staining with GelCode Blue Stain (Thermo Fisher Scientific) (supplementary material Fig. S2).

### Animal maintenance

CAAG-EGFP (K268Q)-GPI transgenic mice were screened by PCR of siblings using tail DNA as template with the following primers: 5'-TTCTTCAAGGACGACGCGCAACTACAAGACC-3' and 5'-GTCACGAACTCCAGCAGGACCATGTGATCG-3'. *Lcn2* knockout mice were screened by PCR using 5'-GGTTTGGTGGCAGGCTATTA-3' and 5'-CAGAGTGGCTTTCCCCATAA-3' for the wild-type allele, and 5'-TGCTCCTGCCGAGAAAAGTAT-3' and 5'-CTCTTCTCTCCAGCACAC-3' for the knockout allele. These transgenic and knockout mice are based on the C57BL/6 genetic background. All animals were housed in a specific pathogen-free (SPF) grade facility and all experiments were approved by the Animal Experiment Committees of the Institute for Frontier Medical Sciences and Kyoto University.

### Sperm collection, incubation, GM1 staining and observation

We used human tubular fluid (HTF)-based medium (101.61 mM NaCl, 4.69 mM KCl, 0.2 mM MgSO<sub>4</sub>, 0.4 mM KH<sub>2</sub>PO<sub>4</sub>, 6.42 mM CaCl<sub>2</sub>, 25 mM NaHCO<sub>3</sub>, 2.77 mM glucose, 3.4 μg/ml sodium lactate, 0.34 mM sodium pyruvate, 0.2 mM penicillin G sodium salt, 0.03 mM streptomycin and 0.4 μl 0.5% Phenol Red) supplemented with 1 mg/ml polyvinyl alcohol (PVA) (Sigma) (HTF-PVA medium) for sperm incubation and IVF. To induce *in vitro* fertility, HTF-based medium was supplemented with 40 μg/ml recombinant LCN2, 4 mg/ml BSA (Sigma) or 0.45 mM M-β-CD (Sigma) (HTF-PVA-LCN2, HTF-BSA or HTF-PVA-M-β-CD media). Sperm from the cauda epididymis were incubated in these media for 120 min; more than 90% of sperm were motile even after this incubation time. After incubation, 10 mM EDTA was added to the samples and they were spread on glass slides followed by air drying and fixation with methanol. To visualize GM1, AlexaFluor 594-conjugated CTB (Molecular Probes) was applied to the samples. To observe the state of EGFP (K268Q)-GPI *in vivo*, ejaculated sperm were collected from the ampulla of oviducts by flushing with HTF-PVA. More than 90% of sperm were motile in the ampulla.

### Calcium ionophore treatment for inducing AR

A 1 mM A23187 calcium ionophore (Sigma) stock solution was prepared with dimethyl sulfoxide (DMSO, Sigma). Epididymal sperm were incubated in HTF-PVA or HTF-PVA-LCN2 for 120 min and then further incubated by adding 10 μM A23187 for 60 min.

### PKA or PI3K inhibitor treatments

Epididymal sperm were incubated in HTF-PVA-LCN2 supplemented with 1.0 μM KT5720 PKA inhibitor (Wako Chemicals) or 5.0 μM AS605240 PI3K inhibitor (Wako Chemicals) for 120 min, fixed with methanol and stained with AlexaFluor 594-conjugated CTB. The LIVE/DEAD Sperm Viability Kit (Molecular Probes) was used to examine sperm viability following the manufacturer's protocol.

### Immunostaining of IZUMO1 to examine the AR

Sperm were fixed with 4% neutral buffered formalin, contacted with a rat monoclonal antibody against mouse IZUMO1 (Inoue et al., 2008; Satouh et al., 2012) and then visualized with AlexaFluor 594-conjugated rabbit anti-rat IgG (Molecular Probes). Sperm were observed under a fluorescence microscope (Olympus).



### In vitro fertilization

Adult C57BL/6J females (more than 10 weeks old) were superovulated by injecting them with 6.7 IU of pregnant mare serum gonadotropin (Teikoku Zoki, Japan) followed 48 h later with 6.7 IU of human chorionic gonadotropin (Teikoku Zoki). Ovulated eggs surrounded by a cumulus mass were collected from the oviducts 16 h after the second injection. Eggs with cumuli were incubated in 200  $\mu$ l HTF-PVA and overlaid with mineral oil. Sperm from the cauda epididymis were preincubated in 100  $\mu$ l HTF-PVA, HTF-PVA-LCN2, HTF-BSA or HTF-PVA-M- $\beta$ -CD for 2 h and then added to the egg drop at a final concentration of  $\sim 1.0 \times 10^5$  sperm/ml. Eggs were washed with modified Whitten's medium (mWM; 109.51 mM NaCl, 4.78 mM KCl, 1.19 mM MgSO<sub>4</sub>, 1.19 mM KH<sub>2</sub>PO<sub>4</sub>, 22.62 mM NaHCO<sub>3</sub>, 5.55 mM glucose, 1.49 mM calcium lactate, 0.23 mM sodium pyruvate, 50  $\mu$ M EDTA, 10  $\mu$ M  $\beta$ -mercaptoethanol, 0.2 mM penicillin G sodium salt, 0.03 mM streptomycin, 3 mg/ml BSA and 0.2  $\mu$ l 0.5% Phenol Red) after 7 h contact with the sperm, and then incubated in fresh mWM for another 16 h. To quantitate fertilization, the percentage fertilization value was determined as follows: % fertilization=(number of 2-cell embryos/total number of unfertilized eggs and 2-cell embryos)  $\times$  100. Values are mean  $\pm$  s.d.

### Measurement of cholesterol

Sperm from the cauda epididymis of wild-type mice were incubated in 1 ml HTF-PVA, HTF-PVA-LCN2, HTF-BSA or HTF-PVA-M- $\beta$ -CD for 120 min and then supernatants were collected by centrifugation at 500 *g* for 5 min. The amount of cholesterol in the supernatants was quantified using a colorimetric enzyme assay kit (cholesterol quantitation kit from Biovision) according to the manufacturer's protocol.

### Immunoblotting

UTJ tissues were obtained and homogenized in a buffer comprising 50 mM Tris pH 8.0, 150 mM NaCl and Complete Protease Inhibitor Cocktail (Roche). After centrifugation at 25,000 *g*, the supernatants were collected and assayed for protein content. First, 10  $\mu$ g protein per sample was subjected to SDS-PAGE. Then,  $2.5 \times 10^5$  sperm incubated in HTF-PVA, HTF-PVA-LCN2, HTF-BSA or HTF-PVA-M- $\beta$ -CD for 120 min were boiled in 25  $\mu$ l SDS-PAGE sample buffer and subjected to SDS-PAGE. Gel-separated samples were electrophoretically transferred onto a nitrocellulose membrane. The membranes carrying UTJ sample were probed with rabbit polyclonal antibody against mouse LCN2 (Santa Cruz Biotechnology, sc-50351) and membranes with sperm samples were probed with a mixture of 4G10 Platinum anti-phosphotyrosine (Millipore) and PY20 anti-phosphotyrosine (Invitrogen) antibodies or rabbit polyclonal anti-RKIP antibody (Santa Cruz Biotechnology, sc-28837). Antibody binding was detected and visualized using the ECL Plus system (GE Healthcare). The blot transfer efficiency was checked by staining with Coomassie Brilliant Blue (Sigma) after immunoblotting. Densities of LCN2 or albumin bands of UTJ samples were quantified with a Molecular Devices densitometer.

### Monitoring LCN2 binding

To monitor LCN2 binding to sperm, HTF-PVA was supplemented with 40  $\mu$ g/ml biotinylated recombinant LCN2, and sperm from the cauda epididymis were incubated for up to 120 min; more than 90% of sperm were motile even after this incubation time. After incubation for the indicated time, 10 mM EDTA was added to the samples and they were placed on ice to stop further reaction and sperm swimming. Sperm samples were then spread on a glass slide, air dried and fixed with methanol. LCN2 binding was visualized using AlexaFluor 488-conjugated streptavidin (Molecular Probes). To visualize GM1, AlexaFluor 594-conjugated CTB was added at the same time.

### Lipid-binding assay

Membrane lipid strips (Echelon Bioscience, P-6002) or Immobilon-P transfer membrane (Millipore) spotted with the indicated amounts of 1,2-dipalmitoyl-*sn*-glycero-3-phosphoethanolamine (PPPE, PE-C16:0/C16:0), 1-palmitoyl-2-oleoyl-*sn*-glycero-3-phosphoethanolamine (POPE, PE-C16:0/C18:1), 1,2-distearoyl-*sn*-glycero-3-phosphoethanolamine (SSPE, PE-C18:0/C18:0), 1-palmitoyl-2-hydroxy-*sn*-glycero-3-phosphoethanolamine (lysoPE,

LPE, PE-C16:0/OH) (all Avanti Polar Lipids) and cholesterol (Sigma) were first contacted with 4  $\mu$ g/ml LCN2 in HTF-PVA supplemented with 1 mM ethanolamine (Sigma) for 16 h and then with anti-FLAG antibody M2 (Sigma) for 5 h. Antibody binding was detected and visualized using the ECL Plus system.

### Sperm staining with biotinylated peptides

One milligram of cinnamycin (Sigma) or 30  $\mu$ g recombinant LCN2 was biotin conjugated with EZ-Link NHS-LC-Biotin (Thermo Fisher Scientific) according to the manufacturer's protocol. After 120 min of incubation on ice, the reaction was terminated by adding 1 M lysine (Sigma). Excess biotin reagent was removed for cinnamycin using PepClean C-18 spin columns (Thermo Fisher Scientific) or for LCN2 using a Microcon Ultracel YM-10 centrifugal filter device (Millipore). Sperm samples smeared on glass were air dried and fixed with methanol. Biotinylated cinnamycin or LCN2 was diluted with HTF-PVA to 2  $\mu$ g/ml and applied to the sample. For the competition assay, 0.1 mg/ml final concentration of unlabeled cinnamycin was added to biotinylated LCN2 samples. Peptide binding was visualized using AlexaFluor 488-conjugated streptavidin (Molecular Probes).

### Statistical analysis

All data for statistical analyses are displayed in supplementary material Table S2. Differences between two groups or multiple means were analyzed by *t*-test using Microsoft Excel software or the ANOVA4 website, respectively. Statistical significance was defined as  $P < 0.05$ .

### Acknowledgements

We thank M. Okabe and T. Kinoshita for helpful discussions; and M. Okabe for providing anti-IZUMO1 antibody.

### Competing interests

The authors declare no competing financial interests.

### Author contributions

H.W., T.T., K.S. and T.B. performed experiments; H.T. and T.W.M. provided experimental materials; N.N. analyzed data; and G.K. designed the research, analyzed data and wrote the paper.

### Funding

This work was supported by grants from the Ministry of Education, Science, Sports and Culture of Japan and the Fujiwara Foundation.

### Supplementary material

Supplementary material available online at <http://dev.biologists.org/lookup/suppl/doi:10.1242/dev.105148/-DC1>

### References

- Åkerstrom, B., Flower, D. R. and Salier, J.-P. (2000). Lipocalins: unity in diversity. *Biochim. Biophys. Acta* **1482**, 1-8.
- Bailey, J. L. (2010). Factors regulating sperm capacitation. *Syst. Biol. Reprod. Med.* **56**, 334-348.
- Berger, T., Togawa, A., Duncan, G. S., Elia, A. J., You-Ten, A., Wakeham, A., Fong, H. E. H., Cheung, C. C. and Mak, T. W. (2006). Lipocalin 2-deficient mice exhibit increased sensitivity to *Escherichia coli* infection but not to ischemia-reperfusion injury. *Proc. Natl. Acad. Sci. U.S.A.* **103**, 1834-1839.
- Costello, S., Michelangeli, F., Nash, K., Lefievre, L., Morris, J., Machado-Oliveira, G., Barratt, C., Kirkman-Brown, J. and Publicover, S. (2009). Ca<sup>2+</sup>-stores in sperm: their identities and functions. *Reproduction* **138**, 425-437.
- Coy, P., Garcia-Vazquez, F. A., Visconti, P. E. and Aviles, M. (2012). Roles of the oviduct in mammalian fertilization. *Reproduction* **144**, 649-660.
- Elangovan, N., Lee, Y.-C., Tzeng, W.-F. and Chu, S.-T. (2004). Delivery of ferric ion to mouse spermatozoa is mediated by lipocalin internalization. *Biochem. Biophys. Res. Commun.* **319**, 1096-1104.
- Flo, T. H., Smith, K. D., Sato, S., Rodriguez, D. J., Holmes, M. A., Strong, R. K., Akira, S. and Aderem, A. (2004). Lipocalin2 mediates an innate immune response to bacterial infection by sequestering iron. *Nature* **432**, 917-921.
- Flower, D. R. (1996). The lipocalin protein family: structure and function. *Biochem. J.* **318**, 1-14.
- Gadella, B. M. and Harrison, R. A. P. (2000). The capacitating agent bicarbonate induces protein kinase A-dependent changes in phospholipid transbilayer behavior in the sperm plasma membrane. *Development* **127**, 2407-2420.

- Goetz, D. H., Holmes, M. A., Borregaard, N., Bluhm, M. E., Raymond, K. N. and Strong, R. K. (2002). The neutrophil lipocalin NGAL is a bacteriostatic agent that interferes with siderophore-mediated iron acquisition. *Mol. Cell* **10**, 1033-1043.
- Ikawa, M., Inoue, N., Benham, A. M. and Okabe, M. (2010). Fertilization: a sperm's journey to and interaction with the oocyte. *J. Clin. Invest.* **120**, 984-994.
- Inoue, N., Ikawa, M. and Okabe, M. (2008). Putative sperm fusion protein IZUMO and the role of N-glycosylation. *Biochem. Biophys. Res. Commun.* **377**, 910-914.
- Jin, M., Fujiwara, E., Kakiuchi, Y., Okabe, M., Satouh, Y., Baba, S. A., Chiba, K. and Hirohashi, N. (2011). Most fertilizing mouse spermatozoa begin their acrosome reaction before contact with the zona pellucida during in vitro fertilization. *Proc. Natl. Acad. Sci. U.S.A.* **108**, 4892-4896.
- Lee, Y.-C., Elangovan, N., Tzeng, W.-F. and Chu, S.-T. (2005). Mouse uterine 24p3 protein as a suppressor of sperm acrosome reaction. *Mol. Biol. Rep.* **32**, 237-245.
- Makino, A., Baba, T., Fujimoto, K., Iwamoto, K., Yano, Y., Terada, N., Ohno, S., Sato, S. B., Ohta, A., Umeda, M. et al. (2003). Cinnamycin (Ro 09-0198) promotes cell binding and toxicity by inducing transbilayer lipid movement. *J. Biol. Chem.* **278**, 3204-3209.
- Minden, A., Lin, A., McMahon, M., Lange-Carter, C., Dérjard, B., Davis, R. J., Johnson, G. L. and Karin, M. (1994). Differential activation of ERK and JNK mitogen-activated protein kinases by Raf-1 and MEKK. *Science* **266**, 1719-1723.
- Satouh, Y., Inoue, N., Ikawa, M. and Okabe, M. (2012). Visualization of the moment of mouse sperm-egg fusion and dynamic localization of IZUMO1. *J. Cell Sci.* **125**, 4985-4990.
- Signorelli, J., Diaz, E. S. and Morales, P. (2012). Kinases, phosphatases and proteases during sperm capacitation. *Cell Tissue Res.* **349**, 765-782.
- Smith, T. T. and Yanagimachi, R. (1990). The viability of hamster spermatozoa stored in the isthmus of the oviduct: the importance of sperm-epithelium contact for sperm survival. *Biol. Reprod.* **42**, 450-457.
- Travis, A. J. and Kopf, G. S. (2002). The role of cholesterol efflux in regulating the fertilization potential of mammalian spermatozoa. *J. Clin. Invest.* **110**, 731-736.
- Visconti, P. E. (2009). Understanding the molecular basis of sperm capacitation through kinase design. *Proc. Natl. Acad. Sci. U.S.A.* **106**, 667-668.
- Visconti, P. E., Bailey, J. L., Moore, G. D., Pan, D., Olds-Clarke, P. and Kopf, G. S. (1995). Capacitation of mouse spermatozoa. I. Correlation between the capacitation state and protein tyrosine phosphorylation. *Development* **121**, 1129-1137.
- Wassarman, P. M. and Litscher, E. S. (2001). Towards the molecular basis of sperm and egg interaction during mammalian fertilization. *Cells Tissues Organs* **168**, 36-45.
- Wassarman, P. M. and Litscher, E. S. (2008). Mammalian fertilization is dependent on multiple membrane fusion events. *Methods Mol. Biol.* **475**, 99-113.
- Watanabe, H. and Kondoh, G. (2011). Mouse sperm undergo GPI-anchored protein release associated with lipid raft reorganization and acrosome reaction to acquire fertility. *J. Cell Sci.* **124**, 2573-2581.
- Yanagimachi, R. (1988). Mammalian fertilization. In *The Physiology of Reproduction* (ed. E. Knobil and J. D. Neil), vol. 1, pp. 135-173. New York: Raven Press.
- Yanagimachi, R. (2009). Germ cell research: a personal perspective. *Biol. Reprod.* **80**, 204-218.
- Zhao, M. (2011). Lantibiotics as probes for phosphatidylethanolamine. *Amino Acids* **41**, 1071-1079.
- Zhao, H., Konishi, A., Fujita, Y., Yagi, M., Ohata, K., Aoshi, T., Itagaki, S., Sato, S., Narita, H., Abdelgelil, N. H. et al. (2012). Lipocalin 2 bolsters innate and adaptive immune responses to blood-stage malaria infection by reinforcing host iron metabolism. *Cell Host Microbe* **12**, 705-716.